Effects of Deep Optic Nerve Head Structures on Bruch's Membrane Opening- Minimum Rim Width and Peripapillary Retinal Nerve Fiber Layer

MITSUKI KAMBAYASHI, HITOMI SAITO, MAKOTO ARAIE, NOBUKO ENOMOTO, HIROSHI MURATA, TSUTOMU KIKAWA, KAZUHISA SUGIYAMA, TOMOMI HIGASHIDE, ATSUYA MIKI, AIKO IWASE, GOJI TOMITA, TORU NAKAZAWA, MAKOTO AIHARA, KYOKO OHNO-MATSUI, TAE-WOO KIM, CHRISTOPHER KAI SHUN LEUNG, LINDA M. ZANGWILL, AND ROBERT N. WEINREB

• PURPOSE: To explore the effects of deep optic nerve head (ONH) structures on Bruch's membrane opening (BMO)-minimum rim width (MRW) and peripapillary retinal nerve fiber layer thickness (pRNFLT) in healthy eyes.

• DESIGN: Prospective cross-sectional study.

• METHODS: Two hundred five healthy eyes of 141 subjects (mean ± standard deviation of age and axial length (AXL): 46.9 ± 10.0 years and 24.79 ± 1.15 mm) were enrolled. Best fit multivariable linear mixed models identified factors associated with BMO-MRW and pRNFLT. Explanatory variables included age, gender, AXL, BMO and anterior scleral canal opening (ASCO) area and ovality, magnitude of BMO and ASCO shift, peripapillary choroidal thickness, lamina cribrosa (LC) parameters, prelaminar thickness, and peripapillary scleral (PPS) angle.

• RESULTS: Thinner BMO-MRW was associated with older age, smaller ASCO/BMO offset magnitude, larger BMO area, thinner prelaminar thickness, deeper LC, and thinner pRNFLT ($P = .011$, $<.001$, $.004$, $<.001$, $<.001$, $<.001$ respectively). Thinner pRNFLT was associated with shorter AXL, smaller ASCO area, a more posteriorly bowed PPS, shallower LC and thinner BMO-MRW. ($P = .030$, $.002$, $.035$, $.012$, $<.001$ respectively)

• CONCLUSIONS: BMO-MRW and pRNFLT were influenced by several deep ONH structures such as BMO and ASCO position shift, BMO or ASCO area, prelaminar thickness, PPS bowing and LC depth in addition to patient characteristics such as age and AXL. The degree and/or direction of associations varied between deep ONH structures and BMO-MRW or pRNFLT. Despite both BMO-MRW and pRNFLT being surrogate parameters for RGC loss, a complex relationship with ONH deep-layer morphology was indicated. (Am J Ophthalmol 2024;263: 99–108.

AJO.com Supplemental Material available at AJO.com.

Accepted for publication February 13, 2024.

From the Department of Ophthalmology (M.K., H.S., M.A.), Graduate School of Medicine, The University of Tokyo, Tokyo, Japan; Kanto Central Hospital of the Mutual Aid Association of Public School Teachers (M.A.), Tokyo, Japan; Tokyo Teishin Hospital (N.E.), Tokyo, Japan; Center Hospital of the National Center for Global Health and Medicine (H.M.), Tokyo, Japan; R&D Division (T.K.), Topcon Corporation, Tokyo, Japan; Department of Ophthalmology (K.S., T.H.), Kanazawa University Graduate School of Medical Sciences, Kanazawa, Japan; Department of Innovative Visual Science (A.M.), Osaka University Graduate School of Medicine, Osaka, Japan; Department of Myopia Control Research (A.M.), Aichi Medical University Medical School, Nagakute, Japan; Tajimi Iwase Eye Clinic (A.I.), Tajimi, Japan; Department of Ophthalmology (G.T.), Toho University Ohashi Medical Center, Tokyo, Japan; Department of Ophthalmology (T.N.), Graduate School of Medicine, Tohoku University, Sendai, Japan; Department of Ophthalmology and Visual Science (K.O.-M.), Tokyo Medical and Dental University, Tokyo, Japan; Department of Ophthalmology (T.-W.K.), Seoul National University College of Medicine, Seoul National University Bundang Hospital, Seongnam, Korea; Department of Ophthalmology, LKS Faculty of Medicine (C.S.K.L.), the University of Hong Kong, Hong Kong Special Administrative Region, China; Hamilton Glaucoma Center, Shiley Eye Institute, and the Viterbi Family Department of Ophthalmology (L.M.Z., R.N.W.), University of California San Diego, La Jolla, CA, United States

Inquires to Hitomi Saito, Department of Ophthalmology, Graduate School of Medicine, The University of Tokyo, Bunkyo-ku, Tokyo, Japan.; e-mail: hitomi8678@gmail.com

Glaucoma is a chronic neurodegenerative disease in which apoptosis of retinal ganglion cells (RGCs) lead to axonal loss and atrophy of retinal nerve fiber layer (RNFL). Degeneration of RGCs observed in histological studies in human eyes with glaucoma is highly associated with the degree of visual field loss.[1] Since glaucoma is an irreversible condition with extensive visual function loss in its advanced stages, accurate assessment of RGC function is essential in glaucoma management. However, quantitatively evaluating the number of RGCs *in vivo* is currently not feasible in clinical practice. Using surrogate methods instead to measure RGC loss is widely used in glaucoma management.

Optical coherence tomography (OCT) is the preferred imaging technology used to quantify neuroretinal rim and peripapillary RNFL thickness (pRNFLT) thinning in glau-

0002-9394/$36.00
https://doi.org/10.1016/j.ajo.2024.02.017

TABLE 1. Exclusion Criteria

Contraindication to Pupillary Dilation
Narrow angle (Shaffer grade ≤ 2)
Glaucoma Hemifield Test "Outside normal limits" and/or PSD <1%
Unreliable HFA results (fixation loss or false negative > 20%, false positive > 15%)
Optic nerve or retinal abnormality including glaucoma
Pathologically myopic eyes or its suspects (ie, eyes with optic disc ovality > 1.33 upon fundus observation, inverted optic discs, posterior staphyloma, focal and/or diffuse macular chorioretinal atrophy, intrachoroidal cavitation)
History of intraocular or refractive surgery
Family history of glaucoma
History of ocular or systemic diseases that could affect HFA/OCT results. (ie, clinically significant cataract, diabetic retinopathy and/or maculopathy, age-related macular degeneration, epiretinal membrane)
History of systemic steroid or anticancer drugs, clinically significant hyper- or hypotension (hypertension: treated systolic blood pressure ≥ 150 mm Hg and diastolic pressure ≥ 95 mm Hg; hypotension: treated systolic blood pressure < 100 mm Hg)

HFA = Humphrey Field Analyzer; OCT = optical coherence tomography; PSD = pattern standard deviation.

coma. Bruch's membrane opening (BMO) - minimum rim width (MRW) and pRNFLT are two surrogate parameters measuring RGC loss. BMO-MRW and pRNFLT values of normal subjects have been applied as reference data in assessing glaucomatous structural damage. However, both parameters are known to be influenced by patient characteristics such as age,[2-4] axial length (AXL),[5-7] gender[8,9] and disc size[4,10-12] and these determining factors must be taken into consideration in optimizing our decision whether the values indicate true abnormality when conducting intergroup comparisons. Since glaucomatous optic nerve head (ONH) structural remodeling is not limited to the rim and RNFL but involves the whole ONH structure, including the Bruch's membrane (BM)[13] peripapillary sclera (PPS)[14] and lamina cribrosa (LC),[15] influence of these deep ONH structures adjacent to BMO-MRW and pRNFLT must also be accounted for when evaluating these parameters.

The objective of this study was to explore the effects of deep ONH structures as well as the influence of patient characteristics on BMO-MRW and pRNFLT to better understand the attributes of these essential parameters in glaucoma management.

METHODS

• **PARTICIPANTS:** All subjects were participants enrolled in the Swept-Source OCT (SS-OCT) Myopia and Glaucoma Study.[7,16] Healthy subjects were recruited using identical inclusion criteria from 8 institutions (Kanazawa University, Osaka University, Tajimi Iwase Eye Clinic, Toho University Ohashi Medical Center, Tohoku University, Seoul National University Bundang Hospital, University of California San Diego and Hong Kong Eye Hospital). Study protocols were approved by the institutional review board of Kanto Central Hospital (R1–06–005) and adhered to the tenets of the Declaration of Helsinki. All patients provided written informed consent before participation in the study.

Self-reported 30 to 70 -year-old healthy volunteers were included. Ocular examinations, including refraction and corneal radius of curvature measurements (ARK-900; NIDEK), best-corrected visual acuity (BCVA) measurements with the 5-meter Landolt chart, AXL measurements (IOL Master; Carl Zeiss Meditec, Inc.), slit-lamp examination, intraocular pressure (IOP) measurements with Goldmann applanation tonometry, dilated fundoscopy, fundus photography, stereophotography and visual field testing with Humphrey Field Analyzer (HFA) 24–2 Swedish Interactive Threshold Algorithm Standard program (Carl Zeiss Meditec, Inc.) were performed at the first visit.

Inclusion criteria for of this study were (1) spherical equivalence (SE) ≤ +1D, astigmatism < 2D, (2) AXL < 28 mm, (3) BCVA >20/25, and (4) attainment of good quality of OCT images (manufacturer recommended criteria of image quality score > 40) and fundus photographs. A healthy eye had no abnormal findings upon complete ophthalmologic assessments, including slit-lamp and fundus examinations, IOP < 21 mm Hg, an open angle, normal optic disc appearance based on clinical stereoscopic examination and fundus photographs (by MA, AI, GT, KOM) and no abnormal HFA results. Exclusion criteria are summarized in Table 1. If one eye of a subject met the exclusion criteria, both eyes were excluded from the study.

• **SWEPT-SOURCE OCT MEASUREMENTS:** Details of OCT image acquisition and measurement of ONH structures have been reported previously.[7] In brief, the ONH and macula of all subjects were imaged by a SS-OCT (DRI OCT Triton; Topcon, Inc.). 6.0 × 6.0 mm ONH raster scans, 24-line BMO-centered radial scans (8 B-scan averaging) and 12.0 × 9.0 mm wide raster scans including both the ONH and macula were obtained for each subject. Magnification corrections were made using a modified Littmann's equa-

tion[17] provided by the manufacturer based on refractive error, corneal radius, and AXL. pRNFLT and peripapillary choroidal thickness (pChT) were measured upon a magnification corrected 3.4 mm diameter BMO-centered annulus. The retinal pigment epithelium (RPE) edge, BMO and anterior scleral canal opening (ASCO) were manually segmented on radial scans reconstructed from raster scans by two experienced examiners (HS, MK). BMO-MRW was measured as the shortest distance between the BMO and peripapillary inner limiting membrane upon each reconstructed radial scan. The average of the 24 BMO-MRW measurements were used for analysis. Other parameters measured from the OCT scans were BMO area/ovality, ASCO area/ovality, ASCO/BMO offset magnitude (representing the magnitude of ASCO centroid misalignment in reference to the BMO centroid, Supplemental Figure 1), ASCO/BMO offset direction (representing the direction of misalignment of ASCO centroid in reference to the BMO centroid, Supplemental Figure 1) and parapapillary zone (PPZ)+Bruch's membrane (BM)/-BM.

Commercial artificial intelligence software, Reflectivity (Abyss Processing, Singapore) was used for LC parameter measurements.[18,19] Segmentation errors were checked by two experienced ophthalmologists (HS, NE) and eyes with Bruch's membrane, anterior LC surface or peripapillary anterior scleral surface segmentation errors and/or invisibility were excluded from the study. LC depth was defined as the distance between the BMO plane and anterior LC surface at the BMO center. The LC global shape index (LC-GSI) is an index with a numerical value between −1 and 1 quantifying the global shape of the LC anterior boundary.[18] Prelaminar thickness was defined as the minimum distance between the anterior surface of the prelaminar tissue to the anterior surface of the LC. PPS angle is the angle between two extended anterior scleral boundaries defined upon a single horizontal B-scan in the nasal-temporal direction between 1200 μm and 1800 μm from the BMO centroid. (Supplemental Figure 2) A larger angle represents a more posteriorly bowed v-shaped PPS configuration.[14,19]

• **STATISTICAL ANALYSIS:** Statistical analyses were performed with IBM SPSS statistics (version 27; International Business Machines [IBM] Corp.) and the statistical programming language "R" (R V.4.2.2; The Foundation for Statistical Computing). Best fit multivariable linear mixed models taking inter-eye correlations into account were used to explore determinants of BMO-MRW and pRNFLT. Considered explanatory variables were age,[2-4] gender (male/female),[8,9] AXL,[5-7] BMO-MRW, pRNFLT, BMO area,[12] BMO ovality, ASCO area, ASCO ovality, ASCO/BMO offset magnitude, ASCO/BMO offset direction, PPZ+BM, PPZ-BM, pChT, LC depth, LC-GSI, prelaminar thickness and PPS angle. Mixed linear models of all possible combinations of these 16 parameters (2^{16}–1 combinations in all) were generated and the model with the best fit (lowest Akaike information criterion [AIC]) was selected for discussion. Since ASCO/BMO offset magnitude and PPZ-BM were strongly correlated with each other ($R = 0.800$, $P < .0001$),[7] we created two models with PPZ-BM excluded as an explanatory variable from the model when ASCO/BMO offset magnitude was included and vice versa to avoid multicollinearity.[20] Since the best fit models including ASCO/BMO magnitude but not PPZ-BM had lower AICs than models including PPZ-BM but not ASCO/BMO magnitude, we present results from the ASCO/BMO magnitude models as representative data. Bonferroni's correction by the number of included explanatory variables in the best fit models were conducted to account for multiple comparisons.

RESULTS

Data from 230 eyes of 155 healthy subjects were collected. After excluding 25 eyes due to LC and anterior scleral segmentation errors, 205 eyes of 141 subjects were enrolled in the study. Baseline characteristics and results of the SS-OCT derived ONH parameters of the healthy subjects are presented in Table 2. Mean ± standard deviation of age and AXL were 46.9 ± 10.0 years and 24.79±1.15 mm, respectively. About 96% of the subjects were of Eastern Asian descent.

Table 3 presents the best fit linear mixed model results demonstrating the effects of patient characteristics and deep ONH structures on BMO-MRW and pRNFLT of healthy eyes. Thinner BMO-MRW of healthy eyes was associated with older age, smaller ASCO/BMO offset magnitude, larger BMO area, thinner prelaminar thickness, deeper LC, and thinner pRNFLT ($P = .011$, $<.001$, $.004$, $<.001$, $<.001$, $<.001$ respectively). Thinner pRNFLT was associated with shorter AXL, smaller ASCO area, a more posteriorly bowed PPS configuration, shallower LC and thinner BMO-MRW. ($P = .030$, $.002$, $.035$, $.012$, $<.001$ respectively)

DISCUSSION

The results of our study reveal that BMO-MRW and pRNFLT of healthy eyes are influenced by several deep ONH structures such as a shift in BMO and ASCO positions, BMO or ASCO area, prelaminar thickness, PPS bowing and LC depth in addition to previously reported patient characteristics such as age[2-4] and AXL.[5-7] Furthermore, the degree and/or direction of associated ONH structures were different between BMO-MRW and pRNFLT, indicating that consideration of deep ONH structure is indispensable in optimizing the interpretation of these parameters.

OCT based estimation of RGC count has traditionally relied on pRNFLT assessment. Meanwhile, the possibility

TABLE 2. Baseline Characteristics

	205 Eyes of 141 Subjects
Age (years old)	46.9 ± 10.0 (30-71)
Gender (M/F)	M: 66 F: 75
R/L	R: 106 L: 99
Spherical equivalent (diopter)	−3.09±2.41 (−9.13∼+1.00)
Axial length (mm)	24.79±1.15 (22.20-27.43)
Mean Deviation (dB)	−0.22±1.14 (−3.48∼2.29)
BMO-MRW (μm)	290.8 ± 49.8 (185.7-435.1)
pRNFLT (μm)	106.0 ± 9.1 (79.0-126.6)
BMO area (mm^2)	2.16±0.55 (1.08-4.12)
BMO ovality	1.12±0.07 (1.01-1.55)
ASCO area (mm^2)	2.81±0.58 (1.42-5.01)
ASCO ovality	1.15±0.11 (1.02-2.11)
ASCO/BMO offset magnitude (μm)	230.8 ± 154.4 (2.8-675.8)
ASCO/BMO offset direction (°)	162.6 ± 45.7 (5.3-312.5)
PPZ+BM (mm^2)	0.74±0.55 (0.12-4.88)
PPZ-BM (mm^2)	0.24±0.33 (0-1.68)
pChT (μm)	138.8 ± 55.4 (54.0-341.4)
LC depth (μm)	429.8 ± 97.9 (115.3-712.8)
LC-GSI	−0.79±0.21 (−1∼0.28)
Prelaminar thickness (μm)	140.6 ± 93.3 (20-440)
PPS angle (°)	6.5 ± 4.2 (−2.0∼22.0)

Values shown as average±standard deviation; () range.

ASCO = anterior scleral canal opening; BM = Bruch's membrane; BMO = Bruch's membrane opening; F = female; L = left; LC = lamina cribrosa; LC-GSI = LC global shape index; M = male; MRW = minimum rim width; pChT = peripapillary choroidal thickness; PPS = peripapillary sclera; PPZ = parapapillary zone; pRNFLT = peripapillary retinal nerve fiber layer thickness; R = right.

that neuroretinal rim changes precede pRNFLT thinning in the earlier stages of glaucoma has been reported,[21] suggesting the usefulness of evaluating the rim structure as a more direct method for quantifying RGC loss. The use of BMO-MRW has been proposed as one such parameter based on an OCT identified landmark.[22] Although BMO- MRW and pRNFLT are theoretically both parameters assessing the viability of the same RGC axons, they are known to have varying characteristics, indicating different representation of the same structure.[3-7,10-12,23] Our study explored determinants of these two parameters in detail by taking deep ONH structures into consideration to better understand the characteristics of these commonly used glaucoma diagnostic parameters.

Older age was associated with thinner BMO-MRW in agreement with previous reports.[2,3] Although age was not selected as a determinant for pRNFLT in multivariable analysis, univariable analysis revealed a similar trend. (nonstandardized regression coefficient −0.092, $P = .226$) This weak trend was confirmatory of a stronger correlation between age and BMO-MRW in comparison with pRNFLT from earlier reports[2,3] and may have been amplified because of the exclusion of subjects older than 70 in our study cohort. Our results confirm the necessity of age correction of BMO- MRW and pRNFLT and that BMO-MRW may be a more sensitive parameter to evaluate age-related RGC loss in healthy eyes.

Longer AXL was not associated with BMO-MRW but was associated with thicker pRNFLT in our study in accordance with prior reports including studies conducted on normal Asian eyes.[7,12] Thickening of the temporal pRNFLT after correction for magnification error in normal eyes with longer AXL is thought to be a result of temporal deviation of the retinal vessels.[5-7] Both BMO- MRW and pRNFLT consist of not only RNFL but of also retinal vasculature and glial contents[21,24] which may dilute their predictive ability for RGC axon degeneration. However, since the average pRNFLT is approximately one third of that of BMO-MRW, retinal vessels account for a higher percentage in pRNFLT and its values are expected to be more strongly influenced by retinal vessel positions.[25] These results suggests that BMO-MRW may have an advantage in quantifying RGC loss in myopic eyes more likely to have vessel position deviations. On the other hand, BMO-MRW values were strongly associated with the shift in BMO and ASCO positions[7] which is clinically equivalent to the presence of PPZ-BM (otherwise known as parapapillary gammazone[26]). This association can be partially explained by a phenomenon termed as peripapillary nerve fiber elevation (pNFE) which has been reported in cross-sectional studies

TABLE 3. Best Fit Multivariable Linear Mixed Models With BMO-MRW and pRNFLT as Response Variables

	BMO-MRW				pRNFLT			
	Standardized Regression Coefficient	Nonstandardized Regression Coefficient	Standard Error	*P*-Value[a]	Standardized Regression Coefficient	Nonstandardized Regression Coefficient	Standard Error	*P*-Value[a]
Age	**−8.293**	**−0.827**	**0.248**	**.011**				
Axial length					**2.162**	**1.8750**	**0.648**	**.030**
ASCO/BMO offset magnitude	**15.080**	**0.100**	**0.173**	**<.001**				
BMO area	**−11.375**	**−20.652**	**5.702**	**.004**	1.902	3.454	1.300	.058
ASCO area	−8.818	−15.185	5.562	.069	**2.813**	**4.844**	**1.288**	**.002**
Prelaminar thickness	**15.524**	**0.166**	**0.026**	**<.001**				
PPS angle					**−1.624**	**−0.389**	**0.137**	**.035**
LC depth	**−20.117**	**−0.205**	**0.032**	**<.001**	**2.025**	**0.021**	**0.006**	**.012**
BMO-MRW		**n/a**			**3.073**	**0.062**	**0.013**	**<.001**
pRNFLT	**10.254**	**1.121**	**0.275**	**<.001**		**n/a**		
pChT	8.010	0.145	0.057	.115				
BMO ovality						−8.519	5.759	.990
ASCO/BMO offset direction	4.470	0.098	0.044	.277				
LC-GSI	2.635	12.483	8.008	.999				

Bold letters: statistically significant *P*-values.

ASCO = anterior scleral canal opening; BMO = Bruch's membrane opening; LC = lamina cribrosa; LC-GSI = LC global shape index; MRW = minimum rim width; pChT = peripapillary choroidal thickness; PPS = peripapillary sclera; pRNFLT = peripapillary retinal nerve fiber layer thickness.

[a] *P*-values after Bonferroni's correction by the number of included explanatory variables.

of normal eyes with long AXL and large PPZs[27,28] as well as in a longitudinal study of healthy children developing myopia.[29] As the temporal BM is shifted temporally in reference to the sclera with AXL elongation in eyes with PPZ-BMs, the nasal neural canal opening becomes crowded and deformed.[29] This leads to an elevation of the nasal rim NFL as can be seen in Figure. However, nasal pRNFLT was not associated with AXL in a previous study.[7] This is most likely because pRNFLT values are measured at a farther distance from the rim structure. Our results demonstrate that both BMO- MRW and pRNFLT values need to be interpreted with caution in myopic eyes because they are influenced by different factors.

ONH size is another well-known influential factor on BMO- MRW and pRNFLT values.[4,10-12] ONH size has traditionally been determined by the ONH margin determined on optic disc photographs. However, with the advancement of OCT technology, we now know that the photographically-derived ONH margins do not have consistent OCT determined anatomical foundations but are rather a combination of BMO and ASCO borders.[22,30] Based on this, we selected OCT defined BMO and ASCO areas as surrogate parameters defining ONH size. pRNFLT is generally known to become thinner in eyes with smaller ONH.[4] Since pRNFLT decreases with distance from the ONH edge,[4] pRNFLT of smaller ONHs are measured at a farther distance from the ONH edge when using a fixed measurement circumference from the disc (BMO) center, resulting in smaller values. However, BMO-MRW, measured at the rim region demonstrates a reverse relationship with ONH size.[10,11] Assuming that the same amount of RGC axons traverse the rim in ONHs with varying size, rim tissue will be expected to be more crowded at the rim region in small ONHs, resulting in thicker BMO-MRW values. The inverse correlation between BMO-MRW and BMO area was in agreement with previous findings.[12] No study has reported on the direct relationship between pRNFLT with ASCO area but the positive correlation found in our results using OCT-defined structural parameters were compatible with past reports exploring relationships with photographically- determined ONH size.[4] Although both parameters were influenced by ONH size, BMO-MRW may be easier to correct for ONH size because the rate of pRNFLT thinning with distance from disc edge is not uniform among sectors.[4] It is also important that the relationships between ONH size and pRNFLT and BMO-MRW in our study were considered taking other confounding factors of ONH size such as AXL[7] and LC depth.[31,32]

Our results revealed that a thinner prelaminar thickness was associated with thinner BMO-MRW while a more posteriorly bowed PPS configuration was associated with thinner pRNFLT. Both thin prelaminar thickness and posteriorly bowed PPS angles have been reported to be observed in glaucomatous eyes,[14,33,34] suggesting that the association of these structural changes may be a sign of very early

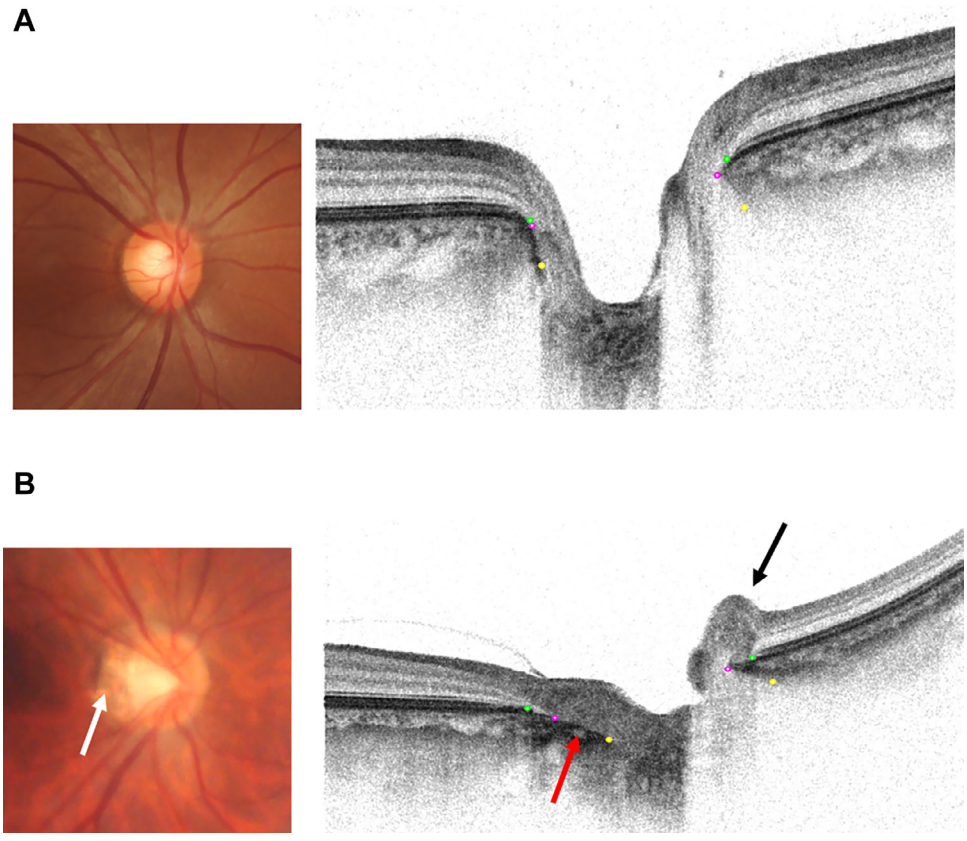

FIGURE. Peripapillary nerve fiber elevation (pNFE) in long axial length (AXL) eyes with parapapillary zone without Bruch's membrane (PPZ-BM). A. Emmetropic eye with AXL of 22.67 mm. No PPZ-BM is observed on the photograph and the disposition of Bruch's membrane opening (BMO; pink dots) and anterior scleral canal opening (ASCO; yellow dots) observed on the OCT image is minimal. No irregularity observed in the nasal rim structure. B. Myopic eye with AXL of 27.27 mm. Typical PPZ-BM is observed on the temporal edge of the optic nerve head photograph. (white arrow) BMO is dispositioned temporally in reference to the ASCO in the PPZ-BM region on the OCT image. (red arrow) The highly elevated nasal rim is the pNFE (black arrow).

glaucomatous changes in otherwise healthy looking eyes or that these changes are predispositions for glaucoma development. However, the true nature of the relationship between these parameters needs to be explored in more detail in future prospective studies.

A deeper LC depth was associated with thinner BMO-MRW while a shallower LC depth was associated with thinner pRNFLT, presenting conflicting results between the two parameters. There are many histological[35] and OCT studies[15] reporting that LC depth is deeper in glaucomatous eyes. However, since this LC deepening is generally associated with elevated IOP[36-38] or older age[37,38] our investigation of LC depth and BMO-MRW or pRNFLT in a cohort of normal IOP healthy eyes may not demonstrate analogous relationships with glaucomatous eyes. Furthermore, the relationship between LC position and glaucoma is still controversial as can be seen from prior studies reporting variation in direction of LC position displacement during longitudinal follow up and weak or no association with the degree of VF, pRNFLT or BMO-MRW progression.[38,39] Along with prior investigations, our results should be interpreted with caution. However, our results do indicate that once again BMO-MRW and pRNFLT demonstrate varying relationships with its surrounding ONH structures.

Other previously reported influential factors of BMO-MRW and pRNFLT include gender, and arteriosclerotic diseases such as hypertension and cerebral strokes.[8,9,40-42] Reports on association between gender and BMO-MRW or pRNFLT thickness have been inconsistent. Male gender was associated with thinner pRNFLT in two studies.[8,9] However, after correcting for patient characteristics and deep ONH structures, we found no association between sex and BMO-MRW or pRNFLT supporting results from other reports including a cohort of healthy Japanese eyes.[4,12,42] We were not able to assess the relationship between systemic diseases and BMO-MRW or pRNFLT in our study due to the exclusion of subjects with systemic diseases such as clinically significant hypertension and hypotension.

Although BMO-MRW and pRNFLT were significantly correlated with each other, their correlation was not necessarily strong ($R = 0.215$, $P = .011$; Pearson's correlation). This result is reasonable considering the varying associa-

TABLE 4. Summarization and Comments on Factors Associated With BMO-MRW and pRNFLT

	BMO-MRW	pRNFLT	Comments
Age	Thinning with older age	No association	BMO-MRW may be a better surrogate for quantification of age-related RGC loss.
Sex	No association	No association	
Axial length	No association	Thinner in eyes with shorter AXL	Temporal shifting of retinal vessels may affect pRNFLT.
ASCO/BMO offset magnitude	Thicker in eyes with larger shift of BMO and ASCO positions	No association	Nasally displaced retinal vessels in eyes with larger ASCO/BMO offset magnitude (clinically equivalent to larger parapapillary gamma-zone) may lead to overestimation of rim structure. (Figure)
BMO area	Thinner in eyes with smaller BMO area		BMO area, ASCO area as surrogate parameters for disc area. BMO-MRW and pRNFLT are both associated with disc size but in opposite directions.
ASCO area		Thinner in eyes with larger ASCO area	BMO-MRW may be easier to correct for disc size because the rate of pRNFLT thinning with distance from disc edge is not uniform among sectors.
Prelaminar thickness	Thinner in eyes with thinner prelaminar thickness	No association	Possible representation of early glaucomatous changes of healthy-looking eyes or indication of predilection to glaucoma.
PPS angle	No association	Thinner in eyes with posteriorly bowed PPS	
LC depth	Thinner in eyes with deeper LC	Thinner in eyes with shallower LC	BMO-MRW and pRNFLT are both associated with LC depth but in opposite directions. Previous literature on the relationship between LC depth and glaucoma are inconsistent and current results also need to be interpreted with caution.

ASCO = anterior scleral canal opening; BMO = Bruch's membrane opening; LC = lamina cribrosa; MRW = minimum rim width; PPS = peripapillary sclera; pRNFLT = peripapillary retinal nerve fiber layer thickness; RGC = retinal ganglion cell.

tions of the two parameters observed in our results with age, ONH size and other adjacent deep ONH structures. Our results were in concordance with previous studies reporting mild association between the two parameters[2] and the discrepancy may have been even more pronounced in our healthy cohort due to the inclusion of a wide range of AXL which affects both BMO-MRW and pRNFLT but in different ways. Although diagnostic ability and structure-function relationship have been reported to be similar[10,43] or slightly superior with BMO-MRW[44] in comparison to pRNFLT, our results demonstrated that the two parameters represent RGC counts in different manners when the effects of deep ONH structures are considered. Knowledge of the influential factors revealed in our study should create a basis for choosing the optimal parameter to evaluate glaucoma depending on the characteristics of each individual eye. A summarization and comparison of the results for BMO-MRW and pRNFLT are presented in Table 4.

Some limitations of our study are (1) the cross-sectional nature of our study, (2) the use of LC depth referenced on the BMO plane, (3) the exclusion of highly hyperopic eyes (SE> +1D) and extremely highly myopic eyes (AL > 28 mm) and (4) our study population being mostly Asian. Investigation of determinant factors of a certain parameter from cross-sectional data may not necessarily reflect true temporal structure changes. However, we consider the robustness of data range in cross-sectional studies can be a strength in determining associated changes. BMO-based LC depth is known to be more affected by choroidal thickness in comparison to anterior scleral-based measurements.[39] Our analysis considered effects of both age and pChT to determine the best-fit model, but the possibility that our method of LC depth measurement led to the discrepant results between BMO-MRW and pRNFLT remains as a possibility. Hyperopic eyes with moderately elongated AXL may have been overlooked and thus may have introduced a somewhat biased AXL distribution in the current dataset in comparison to that of the general population. However, since the prevalence of strongly hyperopic eyes is relatively low in the Japanese population,[45] and the incidence of myopia-like ONHs in hyperopic eyes is very rare, we anticipate that the impact on our study is small. Eyes with AXL > 28 mm were excluded in our current study to avoid confoundment with pathologically myopic eyes. Finally, pRNFLT and BMO-MRW values as well as their decay rate with age have been reported to differ among races.[40,41,46] We need to note that over 95% of our study subjects were of Eastern Asian descent, leaving the possibility that our results cannot be generalized with healthy cohorts of other races.

In conclusion, our current results indicate that BMO-MRW and pRNFLT are mildly associated with each other,

but that they often have varying associations with its influencing patient characteristics and deep ONH structures. Age, AXL, a shift between BMO and ASCO positions, BMO and ASCO area, prelaminar thickness, PPS bowing and LC depth were associated with either or both BMO-MRW and pRNFLT but the degree or direction of association was discrepant. Despite both BMO-MRW and pRNFLT quantifying the integrity of RGC, our study revealed that they have different characteristics as well as strengths and weaknesses. Although further confirmation of these results is awaited from future longitudinal studies, our current results emphasize the necessity of taking influential deep ONH structures into consideration when interpreting the results of these parameters in glaucomatous eyes to determine the magnitude of RGC damage.

CREDIT AUTHORSHIP CONTRIBUTION STATEMENT

Mitsuki Kambayashi: Writing – original draft, Formal analysis. **Hitomi Saito:** Writing – review & editing, Validation, Supervision, Project administration, Methodology, Funding acquisition, Formal analysis, Data curation, Conceptualization. **Makoto Araie:** Writing – review & editing, Supervision, Project administration, Funding acquisition, Conceptualization. **Nobuko Enomoto:** Data curation. **Hiroshi Murata:** Methodology, Formal analysis. **Tsutomu Kikawa:** Software, Resources, Project administration, Formal analysis, Data curation. **Kazuhisa Sugiyama:** Writing – review & editing, Project administration. **Tomomi Higashide:** Writing – review & editing, Project administration. **Atsuya Miki:** Writing – review & editing, Project administration. **Aiko Iwase:** Writing – review & editing, Project administration. **Goji Tomita:** Writing – review & editing, Project administration. **Toru Nakazawa:** Writing – review & editing, Project administration. **Makoto Aihara:** Writing – review & editing, Project administration. **Kyoko Ohno-Matsui:** Writing – review & editing, Project administration. **Tae-Woo Kim:** Writing – review & editing, Project administration. **Christopher Kai Shun Leung:** Writing – review & editing, Project administration. **Linda M. Zangwill:** Writing – review & editing, Project administration. **Robert N. Weinreb:** Writing – review & editing, Project administration.

Funding/Support: Hitomi Saito: Topcon and Japan Society for the Promotion of Science (Project number: 20K18368)
Atsuya Miki: Council for Science, Technology and Innovation (CSTI), Cross-ministerial Strategic Innovation Promotion Program (SIP) "Innovative AI Hospital System". Christopher Kai Shun Leung: Topcon
Tae-Woo Kim: Topcon. Linda Zangwill: National Eye Institute EY027510, Topcon. Robert Weinreb: Topcon Corporation. Financial Disclosure: Mitsuki Kambayashi: None. Hitomi Saito: Carl Zeiss Meditec, Topcon, Senju, Otsuka, Santen, Kowa, Novartis, Abbvie, Viatris, Sandoz, Rhoto (Honoraria). Makoto Araie: Pfizer, Santen, Topcon, Senju, Aerie, Kowa (Consultants), Pfizer, Senju, Kowa (Honoraria), GSTK-DiscAnalysis (License). Hiroshi Murata: Kowa, Beeline (Royalties). Nobuko Enomoto: None. Tsutomu Kikawa: Topcon (employee). Kazuhisa Sugiyama: Santen, Otsuka, Senju, Kowa, Novartis, Viatris, Bayers, Inami Company (Honoraria). Tomomi Higashide: Alcon Japan, Kowa, Novartis, Santen, Senju, Viatris (Honoraria). Atsuya Miki: Alcon, Ellex, Kowa, Menicon, Nitten, Nitto Medic, Otsuka, Rohto, SEED, Senju, Viatris, Topcon (Honoraria), Santen (Consultant). Aiko Iwase: Topcon Corp (Patent), Carl Zeiss Meditec, CREWT Medical Systems, Heidelberg Engineering, Santen, Senju, Otsuka, Novartis (Honoraria) Santen (Consultant).Goji Tomita: Senju, Viatris, Nitto Medic, Kowa (Honoraria). Toru Nakazawa: Topcon Corp, Nidek, Senju (Grants). Kyoko Ohno-Matsui: Santen, CooperVision (Consultant). Makoto Aihara: Santen, Alcon, Pfizer, Otsuka, HOYA, TOMEY, CREWT Medical systems, Carl Zeiss Meditec, Senju, Novartis, Kowa, Johnson & Johnson, Glaukos, Iridex, Canon (Honoraria) Santen, Alcon, Pfizer, Otsuka, Johnson & Johnson, TOMEY, CREWT medical systems, Senju, Novartis, Kowa, Wakamoto, Glaukos, Ono, Sato (Grants) Santen, Alcon, Kowa, Wakamoto, Glaukos, Astellas, Senju, Pfizer, Otsuka, HOYA, IRIDEX (Consultant) Santen, HOYA, Senju, Kowa (Advisory Board). Tae-Woo Kim: None. Christopher Kai Shun Leung: Carl Zeiss Meditec, Heidelberg Engineering, AIROTA Diagnostics Limited (Patents), Carl Zeiss Meditec, Topcon, Heidelberg Engineering, Tomey, Alcon, Arctic Vision, Janssen, Implandata, iCare (Honoraria), Santen, Alcon, Janssen, AbbVie, Arcscan (Advisory Board), Carl Zeiss Meditec, Santen, Alcon, Janssen, AbbVie, Topcon, Zhaoke Ophthalmology, Tomey (Equipment loan); AIROTA Diagnostics Limited, ACE VR Limited (Other). Linda Zangwill: Heidelberg Engineering, Carl Zeiss Meditec (Grants), Carl Zeiss Meditec (License), Abbvie, Digital Diagnostics (Consultants), Topcon, Optovue, Heidelberg Engineering, Carl Zeiss Meditec (Research instruments). Robert N. Weinreb: Abbvie, Aerie Pharmaceuticals, Alcon, Allergan, Amydis, Editas, Equinox, Eyenovia, Iantrek, Implandata, IOPtic, iStar Medical, Nicox, Santen, TenPoint, Topcon (Consultant); National Eye Institute, National Institute of Minority Health and Health Disparities (Research Support); Heidelberg Engineering, Topcon, Zeiss Meditec, Optovue, Centervue, Zilia (Equipment loan); Zeiss Meditec, Toromedes (Patents). All authors attest that they meet the current ICMJE criteria for authorship.

REFERENCES

1. Kerrigan-Baumrind LA, Quigley HA, Pease ME, et al. Number of ganglion cells in glaucoma eyes compared with threshold visual field tests in the same persons. *Invest Ophthalmol Vis Sci*. 2000;41(3):741–748.
2. Chauhan BC, Danthurebandara VM, Sharpe GP, et al. Bruch's membrane opening minimum rim width and retinal nerve fiber layer thickness in a normal white population: a multicenter study. *Ophthalmology*. 2015;122(9):1786–1794. doi:10.1016/j.ophtha.2015.06.001.
3. Chauhan BC, Vianna JR, Sharpe GP, et al. Differential effects of aging in the macular retinal layers, neuroretinal rim, and peripapillary retinal nerve fiber layer. *Ophthalmology*. 2020;127(2):177–185. doi:10.1016/j.ophtha.2019.09.013.
4. Hirasawa H, Tomidokoro A, Araie M, et al. Peripapillary retinal nerve fiber layer thickness determined by spectral-domain optical coherence tomography in ophthalmologically normal eyes. *Arch Ophthalmol*. 2010;128(11):1420–1426. doi:10.1001/archophthalmol.2010.244.
5. Ueda K, Kanamori A, Akashi A, et al. Effects of axial length and age on circumpapillary retinal nerve fiber layer and inner macular parameters measured by 3 types of SD-OCT In-

struments. *J Glaucoma*. 2016;25(4):383–389. doi:10.1097/ijg.0000000000000216.
6. Savini G, Barboni P, Parisi V, et al. The influence of axial length on retinal nerve fibre layer thickness and optic-disc size measurements by spectral-domain OCT. *Br J Ophthalmol*. 2012;96(1):57–61. doi:10.1136/bjo.2010.196782.
7. Saito H, Kambayashi M, Araie M, et al. Deep optic nerve head structures associated with increasing axial length in healthy myopic eyes of moderate axial length. *Am J Ophthalmol*. 2023;249:156–166. doi:10.1016/j.ajo.2023.01.003.
8. Zhao L, Wang Y, Chen CX, et al. Retinal nerve fibre layer thickness measured by Spectralis spectral-domain optical coherence tomography: the Beijing Eye Study. *Acta Ophthalmol*. 2014;92(1):e35–e41. doi:10.1111/aos.12240.
9. Li D, Rauscher FG, Choi EY, et al. Sex-specific differences in circumpapillary retinal nerve fiber layer thickness. *Ophthalmology*. 2020;127(3):357–368. doi:10.1016/j.ophtha.2019.09.019.
10. Enders P, Adler W, Schaub F, et al. Novel bruch's membrane opening minimum rim area equalizes disc size dependency and offers high diagnostic power for glaucoma. *Invest Ophthalmol Vis Sci*. 2016;57(15):6596–6603. doi:10.1167/iovs.16-20561.
11. Cho HK, Park JM, Kee C. Effect of optic disc size on correlation between Bruch's membrane opening-minimum rim width and peripapillary retinal nerve fibre layer thickness. *Eye (Lond)*. 2019;33(12):1930–1938. doi:10.1038/s41433-019-0525-9.
12. Araie M, Iwase A, Sugiyama K, et al. Determinants and characteristics of bruch's membrane opening and bruch's membrane opening-minimum rim width in a normal Japanese population. *Invest Ophthalmol Vis Sci*. 2017;58(10):4106–4113. doi:10.1167/iovs.17-22057.
13. Lowry EA, Mansberger SL, Gardiner SK, et al. Association of optic nerve head prelaminar schisis with glaucoma. *Am J Ophthalmol*. 2021;223:246–258. doi:10.1016/j.ajo.2020.10.021.
14. Wang X, Tun TA, Nongpiur ME, et al. Peripapillary sclera exhibits a v-shaped configuration that is more pronounced in glaucoma eyes. *Br J Ophthalmol*. 2022;106(4):491–496. doi:10.1136/bjophthalmol-2020-317900.
15. Park SC, Brumm J, Furlanetto RL, et al. Lamina cribrosa depth in different stages of glaucoma. *Invest Ophthalmol Vis Sci*. 2015;56(3):2059–2064. doi:10.1167/iovs.14-15540.
16. Saito H, Ueta T, Araie M, et al. Association of bergmeister papilla and deep optic nerve head structures with prelaminar schisis of normal and glaucomatous eyes. *Am J Ophthalmol*. 2023;257:91–102. doi:10.1016/j.ajo.2023.09.002.
17. Littmann H. Determining the true size of an object on the fundus of the living eye. *Klin Monbl Augenheilkd*. 1988;192(1):66–67 Zur Bestimmung der wahren Grösse eines Objektes auf dem Hintergrund eines lebenden Auges. doi:10.1055/s-2008-1050076.
18. Thakku SG, Tham YC, Baskaran M, et al. A global shape index to characterize anterior lamina cribrosa morphology and its determinants in healthy Indian eyes. *Invest Ophthalmol Vis Sci*. 2015;56(6):3604–3614. doi:10.1167/iovs.15-16707.
19. Fortune B. Pulling and tugging on the retina: mechanical impact of glaucoma beyond the optic nerve head. *Invest Ophthalmol Vis Sci*. 2019;60(1):26–35. doi:10.1167/iovs.18-25837.
20. Farrar DE. Multicollinearity in regression analysis: the problem revisited. *Rev Econ Stats*. 1967;49(1):92–107. doi:10.2307/1937887.
21. Patel NB, Sullivan-Mee M, Harwerth RS. The relationship between retinal nerve fiber layer thickness and optic nerve head neuroretinal rim tissue in glaucoma. *Invest Ophthalmol Vis Sci*. 2014;55(10):6802–6816. doi:10.1167/iovs.14-14191.
22. Reis AS, O'Leary N, Yang H, et al. Influence of clinically invisible, but optical coherence tomography detected, optic disc margin anatomy on neuroretinal rim evaluation. *Invest Ophthalmol Vis Sci*. 2012;53(4):1852–1860. doi:10.1167/iovs.11-9309.
23. Chauhan BC, Burgoyne CF. From clinical examination of the optic disc to clinical assessment of the optic nerve head: a paradigm change. *Am J Ophthalmol*. 2013;156(2):218–227 e2. doi:10.1016/j.ajo.2013.04.016.
24. Ogden TE. Nerve fiber layer of the primate retina: thickness and glial content. *Vision Res*. 1983;23(6):581–587. doi:10.1016/0042-6989(83)90063-9.
25. Yamashita T, Asaoka R, Tanaka M, et al. Relationship between position of peak retinal nerve fiber layer thickness and retinal arteries on sectoral retinal nerve fiber layer thickness. *Invest Ophthalmol Vis Sci*. 2013;54(8):5481–5488. doi:10.1167/iovs.12-11008.
26. Wang YX, Panda-Jonas S, Jonas JB. Optic nerve head anatomy in myopia and glaucoma, including parapapillary zones alpha, beta, gamma and delta: histology and clinical features. *Prog Retin Eye Res*. 2021;83:100933. doi:10.1016/j.preteyeres.2020.100933.
27. Yamashita T, Sakamoto T, Yoshihara N, et al. Peripapillary nerve fiber elevation in young healthy eyes. *Invest Ophthalmol Vis Sci*. 2016;57(10):4368–4372. doi:10.1167/iovs.16-19484.
28. Terasaki H, Yamashita T, Tanaka M, et al. Relationship between funduscopic conus and optic disc factors associated with myopia in young healthy eyes. *Invest Ophthalmol Vis Sci*. 2020;61(2):40. doi:10.1167/iovs.61.2.40.
29. Kim YW, Choi JJ, Girard MJA, et al. Longitudinal observation of border tissue configuration during axial elongation in childhood. *Invest Ophthalmol Vis Sci*. 2021;62(4):10. doi:10.1167/iovs.62.4.10.
30. Sawada Y, Araie M, Shibata H, et al. Optic disc margin anatomic features in myopic eyes with glaucoma with spectral-domain OCT. *Ophthalmology*. 2018;125(12):1886–1897. doi:10.1016/j.ophtha.2018.07.004.
31. Tun TA, Wang X, Baskaran M, et al. Determinants of lamina cribrosa depth in healthy Asian eyes: the Singapore Epidemiology Eye Study. *Br J Ophthalmol*. 2021;105(3):367–373. doi:10.1136/bjophthalmol-2020-315840.
32. Luo H, Yang H, Gardiner SK, et al. Factors influencing central lamina cribrosa depth: a multicenter study. *Invest Ophthalmol Vis Sci*. 2018;59(6):2357–2370. doi:10.1167/iovs.17-23456.
33. Kim DW, Jeoung JW, Kim YW, et al. Prelamina and lamina cribrosa in glaucoma patients with unilateral visual field loss. *Invest Ophthalmol Vis Sci*. 2016;57(4):1662–1670. doi:10.1167/iovs.15-18453.
34. Yazdani S, Naderi Beni A, Pakravan M. Laminar and prelaminar tissue characteristics of glaucomatous eyes using enhanced depth imaging OCT. *Ophthalmol Glaucoma*. 2021;4(1):95–101. doi:10.1016/j.ogla.2020.08.007.
35. Quigley HA, Hohman RM, Addicks EM, et al. Morphologic changes in the lamina cribrosa correlated with neural loss in open-angle glaucoma. *Am J Ophthalmol*. 1983;95(5):673–691. doi:10.1016/0002-9394(83)90389-6.

36. Quigley HA, Addicks EM. Chronic experimental glaucoma in primates. II. Effect of extended intraocular pressure elevation on optic nerve head and axonal transport. *Invest Ophthalmol Vis Sci*. 1980;19(2):137–152.
37. Burgoyne CF, Downs JC, Bellezza AJ, et al. The optic nerve head as a biomechanical structure: a new paradigm for understanding the role of IOP-related stress and strain in the pathophysiology of glaucomatous optic nerve head damage. *Prog Retin Eye Res*. 2005;24(1):39–73. doi:10.1016/j.preteyeres.2004.06.001.
38. Wu Z, Xu G, Weinreb RN, et al. Optic nerve head deformation in glaucoma: a prospective analysis of optic nerve head surface and lamina cribrosa surface displacement. *Ophthalmology*. 2015;122(7):1317–1329. doi:10.1016/j.ophtha.2015.02.035.
39. Vianna JR, Lanoe VR, Quach J, et al. Serial changes in lamina cribrosa depth and neuroretinal parameters in glaucoma: impact of choroidal thickness. *Ophthalmology*. 2017;124(9):1392–1402. doi:10.1016/j.ophtha.2017.03.048.
40. Girkin CA, McGwin Jr G, Sinai MJ, et al. Variation in optic nerve and macular structure with age and race with spectral-domain optical coherence tomography. *Ophthalmology*. 2011;118(12):2403–2408. doi:10.1016/j.ophtha.2011.06.013.
41. Knight OJ, Girkin CA, Budenz DL, et al. Effect of race, age, and axial length on optic nerve head parameters and retinal nerve fiber layer thickness measured by Cirrus HD-OCT. *Arch Ophthalmol*. 2012;130(3):312–318. doi:10.1001/archopthalmol.2011.1576.
42. Mauschitz MM, Bonnemaijer PWM, Diers K, et al. Systemic and ocular determinants of peripapillary retinal nerve fiber layer thickness measurements in the european eye epidemiology (E3) population. *Ophthalmology*. 2018;125(10):1526–1536. doi:10.1016/j.ophtha.2018.03.026.
43. Malik R, Belliveau AC, Sharpe GP, et al. Diagnostic accuracy of optical coherence tomography and scanning laser tomography for identifying glaucoma in myopic eyes. *Ophthalmology*. 2016;123(6):1181–1189. doi:10.1016/j.ophtha.2016.01.052.
44. Chauhan BC, O'Leary N, AlMobarak FA, et al. Enhanced detection of open-angle glaucoma with an anatomically accurate optical coherence tomography-derived neuroretinal rim parameter. *Ophthalmology*. 2013;120(3):535–543. doi:10.1016/j.ophtha.2012.09.055.
45. Sawada A, Tomidokoro A, Araie M, et al. Refractive errors in an elderly Japanese population: the Tajimi study. *Ophthalmology*. 2008;115(2):363–370 e3. doi:10.1016/j.ophtha.2007.03.075.
46. Zangalli CS, Vianna JR, Reis ASC, et al. Bruch's membrane opening minimum rim width and retinal nerve fiber layer thickness in a Brazilian population of healthy subjects. *PLoS One*. 2018;13(12) e0206887. doi:10.1371/journal.pone.0206887.